Evaluation of redundancy analysis to identify signatures of local adaptation

Thibaut CAPBLANCQ[1*], Keurcien LUU[2], Michael G.B. BLUM[2] and Eric BAZIN[1,#]

[1] *Univ. Grenoble Alpes, CNRS, LECA UMR 5553, Grenoble, France*
[2] *Univ. Grenoble Alpes, CNRS, TIMC-IMAG UMR 5525, Grenoble, France*
[#]*Deceased*

* Corresponding author: Thibaut Capblancq, 2233 Rue de la Piscine, 38041 Grenoble Cedex, France. Tel.: +33 (0)4 76 51 36 71, e-mail: thibaut.capblancq@univ-grenoble-alpes.fr

Date: May 18, 2018

Running title: RDA-based procedure for genome scans

ABSTRACT

Ordination is a common tool in ecology that aims at representing complex biological information in a reduced space. In landscape genetics, ordination methods such as principal component analysis (PCA) have been used to detect adaptive variation based on genomic data. Taking advantage of environmental data in addition to genotype data, redundancy analysis (RDA) is another ordination approach that is useful to detect adaptive variation. This paper aims at proposing a test statistic based on RDA to search for loci under selection. We compare redundancy analysis to pcadapt, which is a nonconstrained ordination method, and to a latent factor mixed model (LFMM), which is a univariate genotype-environment association method. Individual-based simulations identify evolutionary scenarios where RDA genome scans have a greater statistical power than genome scans based on PCA. By constraining the analysis with environmental variables, RDA performs better than PCA in identifying adaptive variation when selection gradients are weakly correlated with population structure. Additionally, we show that if RDA and LFMM have a similar power to identify genetic markers associated with environmental variables, the RDA-based procedure has the advantage to identify the main selective gradients as a combination of environmental variables. To give a concrete illustration of RDA in population genomics, we apply this method to the detection of outliers and selective gradients on an SNP data set of *Populus*

trichocarpa (Geraldes *et al.*, 2013). The RDA-based approach identifies the main selective gradient contrasting southern and coastal populations to northern and continental populations in the northwestern American coast.

KEYWORDS: Genome scans - Multivariate analysis - Redundancy analysis – Biological adaptation – Selection – Environmental variables

INTRODUCTION

Natural selection results from environmental pressures. The environment acts simultaneously on several characteristics, and these adaptive characteristics can be determined by a large number of alleles of small effects (Pritchard and Di Rienzo, 2010). Patterns of adaptive variation within species are usually studied through physiological, morphometric and fitness comparisons in common garden experiments. However, this is a difficult and constraining task, which can even be unrealistic to achieve in species with a long generation time. Recently, the development of next-generation sequencing (NGS) technologies has opened the possibility to access to a large amount of genetic variation across the genome. Therefore, relationships between genetic polymorphism, phenotypic variation and environmental variables can now be studied and quantified by in situ approaches (Steane *et al.*, 2014, Vangestel *et al.*, 2018).

41

42 By looking for loci that are either excessively differentiated between
43 populations or significantly associated with environmental gradients, adaptive
44 variation can be detected (Foll and Gaggiotti 2008, Frichot *et al.*, 2013, Vatsiou *et al.*,
45 2015, Duforet-Frebourg *et al.*, 2016, Hoban *et al.*, 2016).

46 In many genome scan procedures, outlier loci are identified based on genetic
47 differentiation, assuming that adaptive alleles have increased genetic differentiation.
48 A common statistic to evaluate genetic differentiation is F_{st} (Lewontin and Krakauer,
49 1973) and many likelihood or Bayesian methods use F_{st}-related statistics to scan
50 genomes for local adaptation (Bazin *et al.*, 2010, De Villemereuil and Gaggiotti, 2015,
51 Foll and Gaggiotti, 2008, Whitlock and Lotterhos, 2015). One limitation of F_{st}-based
52 approaches is that they require defining discrete populations, whereas many species
53 are not structured in different populations but display continuous genetic gradients
54 (Martins *et al*. 2016). In these cases, defining populations can be challenging and can
55 directly interfere with the result of the analysis (Yang *et al.*, 2012).

56 A solution to avoid such an issue is to use individual-based multivariate
57 methods such as PCA that ascertain population structure. Duforet-Frebourg and
58 colleagues (2016) proposed a genome scan method based on PCA (pcadapt), where
59 outlier loci are the ones excessively correlated with one or more ordination axes
60 (Duforet-Frebourg *et al.*, 2016). Simulations show that pcadapt has a similar power

61 to model-based methods under island models and perform better when the
62 simulated demographic model drifts from the island model, for instance under
63 hierarchical population structure or isolation by distance patterns (Luu *et al.*, 2017).
64 Nevertheless, one conundrum of such approaches is the difficulty to interpret
65 ordination axes in terms of ecological meanings. These are usually tight to
66 geographical axes (latitudinal or longitudinal), but they are not necessarily linked to
67 an environmental variable such as temperature, drought, diet habit, etc. When
68 environmental information exists, it has to be used, a posteriori, as a means of
69 interpretation, but it is not involved in the inference process.

70 Genotype-environment association (GEA) methods are based on a different
71 principle than methods based on genetic differentiation; they assume that adaptive
72 loci are significantly associated with environmental variation. These methods aim at
73 detecting alleles that are associated with environmental variables (e.g., temperature
74 and drought) with the idea that these alleles may confer a selective advantage in
75 some environment (Coop *et al.*, 2010, Frichot *et al.*, 2013). Most of these methods
76 only use one predictor variable at a time, which can be problematic when the main
77 selective gradient is unknown or when we want to disentangle multifactorial
78 associations between genetic and environmental variation.

79

80 Some authors have proposed to use a constrained ordination procedure such

81 as RDA (redundancy analysis) or CAPs (canonical analysis of principal coordinates)
82 to combine the advantages of both multivariate methods and genotype-environment
83 association procedures (Lasky *et al.*, 2012, DeKort *et al.*, 2014; Steane *et al.*, 2014,
84 Hecht *et al.*, 2015). This family of methods subsequently aligns adaptive variation
85 with environmental data in order to be able to identify the environmental gradients
86 that are the most correlated with adaptive variation. In *Arabidopsis thaliana,* loci
87 involved in adaptation to climate have been found using RDA (Lasky *et al.*, 2012).
88 Outliers were identified as SNPs with the greatest squared loadings along the first
89 RDA axes (i.e., those in the 0.5% tail). RDA can also be used to derive an adaptive
90 index that predicts the performance of individuals in different environmental
91 conditions. Steane *et al.* (2014) applied a similar approach (using canonical analysis
92 of principal coordinates) to *Eucalyptus tricarpa* populations and showed that both
93 detection of adaptive variation with RDA and common garden experiments provided
94 evidence for local adaptation. Finally, in two recent studies, Forester and colleagues
95 (2015 and 2017) tested the power of an RDA-based method for detecting signatures
96 of local adaptation in a heterogeneous landscape (Forester *et al*, 2015) and in
97 comparison with other constrained ordination methods (Forester *et al*, 2017). Using
98 simulations, they found that an RDA-based method has a superior combination of
99 low false positive and high true positive rates when compared to generalized linear
100 models (GLM) or latent factor mixed models (LFMM).

101 In this paper, we build on these previous applications of RDA to develop a
102 statistical test for searching loci under selection. We use simulations and real data
103 sets to shed light on the conditions within which RDA is the most efficient and to
104 document the possibilities given by RDA when studying landscape genomics. We
105 also compare results of a genome scan based on RDA with genome scans obtained
106 with *pcadapt* and LFMM (Frichot et al. 2013, Luu *et al.,* 2017). This investigation
107 gives the opportunity to show the advantages of a constrained ordination method
108 such as RDA in comparison with nonconstrained ordination method (PCA) and
109 univariate genotype-environment association method (LFMM). Finally, to illustrate
110 the pertinence of such a method in a concrete example, we apply it to a *Populus*
111 *trichocarpa* SNP dataset obtained from Geraldes *et al.* (2013). We found a large
112 overlap between the outlier loci detected with RDA and the loci previously detected
113 with *Fst* based methods (Geraldes *et al.*, 2013). In addition, RDA revealed what the
114 main selective gradients are along the natural populations of *Populus trichocarpa* in
115 the northwestern coast of North America.
116

117 # MATERIALS AND METHODS

118 ## 1. Genome scan using an RDA-based approach

119 Redundancy analysis (RDA) was first introduced by Rao (1964). It is the
120 extension of multiple regressions to the modeling of multivariate response data

121 (Legendre and Legendre 2012, section 11.1). The data are separated in two sets, a
122 response matrix Y of the variable to be explained (e.g., species abundance in a set of
123 sites; m sites and n species) and an explanatory matrix X (e.g., a set of environmental
124 variables within each site; m sites and p environment). In the following analysis, loci
125 replace species abundances and individuals replace sites. RDA seeks to project the
126 genetic variation between individuals that is explained by environmental data on a
127 reduced space. RDA assumes that there are linear relationships between the
128 response (Y) and explanatory (X) variables.

129 The analysis starts using a classical RDA procedure performed with the
130 function *rda* of the R package *"vegan"* (Oksanen *et al.*, 2015). An individual genetic
131 dataset is used as the response matrix Y, and a set of environmental variables is used
132 as explanatory matrix X. We assume in the following that genotypes are coded using
133 the values 0,1, or 2 that correspond to homozygote for the most frequent allele,
134 heterozygote and homozygote for the less frequent allele. RDA amounts at
135 constructing a matrix Y' of fitted genetic values estimated from the regression of
136 each locus by the environmental variables and at performing principal component
137 analysis on the matrix Y' (Legendre and Legendre 2012, section 11.1). After this
138 constrained ordination step, we follow the methodology implemented in *pcadapt* to
139 find outlier loci (Luu *et al.,* 2017). First, we recover the loci loadings from the RDA
140 analysis. Only the loadings of the most informative ordination axis are kept for the

141 rest of the procedure. The number of axes used (K) is determined by looking at the
142 amount of information retained on the different axes of the RDA. A Mahalanobis
143 distance D is then computed for each locus to identify loci showing extreme D values
144 compared to the rest of the SNPs. A Mahalanobis distance is a multidimensional
145 generalization of the idea of measuring how many standard deviations is a point
146 from an average point. Computation of the Mahalanobis distance uses the *covRob*
147 function of the "*robust*" R package (Wang et al., 2014). Mahalanobis distances are
148 distributed as chi-squared distribution with K degrees of freedom after correcting
149 with the genomic inflation factor (Luu et al., 2017). Inflation factors are constant
150 values that are used to rescale chi-square statistics in order to limit inflation due to
151 diverse confounding factors (François et al 2016). We then adjust the resulting p-
152 values for the false discovery rate (FDR) by computing q-values with the "qvalue" R
153 package (Dabney and Storey, 2011). A locus is considered as an outlier if its q-value
154 is less than 10%, meaning that 10% or less of the identified outliers could be false
155 positives. The complete procedure is described in Fig. 1 and our R script is available
156 in the supplementary material (Script S1).

157 To evaluate the capacity of the RDA-based approach to detect loci underlying
158 environmental selective pressure, we first test the method with simulated datasets.
159 A total of 100 independent runs of simulations were used (see below for details). We
160 evaluate the power of the procedure based on RDA to detect positive loci (loci

161 simulated under selection) and to return a controlled number of false positives
162 (neutral loci detected as outliers by the analysis). Then, to emphasize the utility of
163 this method, we compared it to the PCA-based procedure implemented in *pcadapt*
164 that does not use environmental variables (Luu *et al.*, 2017). In the same vein, we
165 compare the multivariate RDA-based procedure to LFMM, which is an univariate
166 genotype-environment association method (Frichot *et al.*, 2013). This method
167 processes one environmental variable at a time, whereas we wanted to evaluate to
168 what extent different techniques can disentangle covariation between multiple
169 environmental gradients and multilocus genetic variation. To tackle this issue, we
170 performed the LFMM analysis with a set of composite environmental variables
171 corresponding to the first two PCs of a PCA performed on the environmental
172 simulated variables (Frichot *et al.*, 2013). It gave us orthogonal composite
173 environmental variables for which we tested covariation with genetic variability
174 through the LFMM procedure. The LFMM analysis was launched with only one latent
175 factor (K = 1), taking into account that simulations have been made without any
176 population divergence.
177

178 **2. Simulated data**

179 We used simulations performed with the simuPop python library (Peng *et al.*,
180 2005). A lattice of 8x8 populations is simulated (i.e., 64 populations in total). Each

181 population is initialized with 200 diploid individuals with random genotypes.
182 Migration is set to 0.1, resulting in an isolation-by-distance pattern across the
183 species range. Loci are assumed to be biallelic SNPs. The allele frequency of the
184 whole population is initialized at 0.5. 1000 loci are simulated in total and they are
185 separated in 200 chunks of 5 SNPs in physical linkage with the recombination rate
186 between adjacent loci fixed at 0.1. Three different quantitative traits are coded by a
187 group of 10 different loci (quantitative trait locus, QTL). The first quantitative trait is
188 coded by the loci 1, 11, 21,..., 91. The trait value is simply the sum of the genotype
189 values and therefore can take values between 0 and 20. We add to each trait a
190 random noise (nonheritable variation) drawn from a normal distribution $N(0,2)$. The
191 second quantitative trait is coded by loci 101, 111,..., 191 and the third is coded by
192 loci 201, 211,..., 291. Each quantitative trait is therefore coded by 10 independent
193 SNPs (QTL), resulting in a total of 30 causal SNPs among the 1000. Selection can
194 have an effect on linked loci, for instance, loci 2, 3, 4 and 5 can be impacted by
195 selection on locus 1. However, recombination is high enough (0.1) to expect a limited
196 linkage effect. We have defined 10 different environmental variables. The first one
197 determines the selective pressure on trait 1, the second one on trait 2 and the third
198 one on trait 3. The first environment variable is a quadratic gradient coded by
199 function $env1 = -(\cos(\theta)*(i-3.5))^2 -(\sin\theta)*(j-3.5))^2 + 18$, $\theta = \pi/2$, with i and j being
200 the population indicator on the 8x8 lattice. The second one is a linear plan gradient

201 coded by function *env2* = h*cos(θ)*(i-1) + h*sin(θ)*(j-1) + k with h = 2, $\theta = \pi/4$ and
202 k=3. The third environment variable simulates a coarse environment with value
203 *env*3 = 2 for all populations except population (i,j) = (2,2), (2,3), (3,2), (3,3), (6,2),
204 (6,3), (7,2), (7,3), (2,6), (2,7), (3,6), (3,7), (6,6), (6,7), (7,6), (7,7), for which *env*3 = 18.
205 Env4, env5 and env6 have exactly the same equation as env1, env2 and env3,
206 respectively, except for a noise term explained below. The remaining 4 environment
207 variables are similar to env2 but with different values of h and θ. Env7 has h = 2, θ =
208 0 and k = 3. Env8 has h = 2, $\theta = \pi/4$ and k = 0. Env9 has h = 1, $\theta = \pi/4$ and k=4. Env10
209 has h=0.5, $\theta = \pi/4$ and k = 8. Graphical representation of the mean environmental
210 value is given in Fig. 2. Environmental variables 4, 5 and 6 have, respectively, the
211 same mean value spatial distribution as environmental variables 1, 2 and 3. The
212 environmental equation gives a mean value of the environment variable. To avoid
213 collinearity between environmental variables, we added noise by drawing an
214 environment value within a normal distribution N(μ = env, σ = 1). The fitness for
215 each trait is set to be –exp(x-env)^2/(2*ω^2), with x being the quantitative trait
216 value, *env* the environmental value and ω is the defining selection strength and has
217 been set to 20, which was found to be enough for loci to be often detected. To get the
218 overall fitness for a given individual, the fitness associated with each trait is
219 multiplied. Fitness values are used to determine the number of offspring during the
220 simulations, which have been launched for 500 generations. At the end of the

221 simulation, we sampled 10 individuals per population resulting in 640 individuals
222 with 1000 SNP-like loci.
223
224 **3. Real dataset**
225 The *Populus trichocarpa* dataset is a sample of 424 individuals genotyped on
226 33,070 SNPs from 25 drainages (i.e., topographic units separated by watershed
227 barriers) (Geraldes *et al.*, 2014). Genotyping of each accession was performed with a
228 34K Populus SNP array targeting 34,131 SNPs mostly within (plus 2 kb upstream
229 and downstream) 3543 genes (Geraldes *et al.*, 2013). A total of 21 climatic variables
230 are available on each sampling site (Table S1). From the 33,070 SNPs, we removed
231 the SNPs with missing values and a minor allele frequency below 5% resulting in
232 17,224 SNPs.
233 We explored the adaptive genetic variability of the *Populus trichocarpa*
234 dataset using PCA-based (*pcadapt*) and RDA-based method using the 21
235 environmental variables as explanatory variables (Table S2). Similar to the
236 simulations above, we created two environmental composite variables by keeping
237 the two first axes of a PCA on the 21 environmental variables. We then used the
238 latent factor mixed model (LFMM) procedure on these composite variables and with
239 one latent factor (K=1). We finally compared the list of outliers found with these
240 three approaches to the ones found using *Fst* based methods (Geraldes *et al.*, 2014).

241 We then performed a second RDA with only the loci previously found as
242 outliers (q-values < 0.1). This set of outliers gives an "adaptively enriched genetic
243 space" (Steane *et al*., 2014) and using a second RDA on these specific loci, we can
244 identify the environmental variables that are the most correlated with "putatively"
245 adaptive variation. Using only outlier loci avoids potential interferences brought by
246 the "neutral" genetic variation during the alignment between genetic and
247 environmental variation performed by RDA. We then used the scores of the different
248 *Populus trichocarpa* populations along the first two RDA axes to build composite
249 indexes, which correspond to the main environmental pressures driving adaptive
250 genetic variation. The individuals' scores on the axes of the adaptively enriched
251 genetic RDA can be interpreted as cursors of individual genetic adaptation to the
252 environmental variables associated with these axes. We thus represented the mean
253 RDA1 and RDA2 individual score for each of the 133 populations on a map. It allows
254 visualizing the adaptive landscape across the sampling area.
255

256 # RESULTS

257 **1. Genome scan on simulated dataset using RDA, pcadapt and LFMM**
258 **methods**

259 The procedure was first performed on one simulation (sim1) with pcadapt,
260 RDA and LFMM approaches. To perform RDA, we considered environmental

261 variables 1-10 as explanatory variables. For pcadapt and RDA, we retained the first
262 four ordination axes to compute Mahalanobis distances as indicated by the scree
263 plots (Fig. S1). In parallel, we independently launched LFMM analysis with the first
264 two PCs resulting from a PCA applied to environmental variables (Fig. S2). We then
265 estimate that a locus is considered as an outlier by LFMM if there is a significant
266 correlation with at least one of the two composite variables.

267 The software package *pcadapt* is successful at detecting QTL2 SNPs (Fig. 3
268 topleft) but fails entirely at detecting QTL1 and QTL3 SNPs. The RDA-based
269 approach also detects QTL2 SNPS and most of the QTL1 SNPs in contrast to *pcadapt*
270 (Fig. 3 topright). The LFMM method is also able to detect most of the QTL1 and all
271 the QTL2 SNPs. These SNPs are detected when respectively regressing the genetic
272 dataset with the first and the second environmental composite variables (Fig. 3
273 bottom). For the SNPs associated with QTL3, the three methods have negligible
274 power to detect them.

275 When looking at the projection of each SNP in the RDA space, we can detect
276 links between QTL SNPs and environmental variables (Fig. 4). RDA1 is strongly
277 correlated to env2 and env5 and the QTL2 SNP show extreme scores on this axis
278 compared to the other SNPs, especially the neutral ones (Fig. 4A). RDA2 is also
279 associated with env7, env8, env9 and env10, which had not been used as direct
280 selective drivers during the simulations. RDA3 is correlated to env1 and env4

281 corresponding to QTL1 SNPs and there is also a weak association between RDA4
282 (env3 and env6) and the SNPs associated with QTL3 (Fig. 4B & 3C).
283 When looking at the percentage of environmental variance explained by the
284 RDA and PCA axes, we find that the first four RDA axes explain more variance of each
285 environmental variable than the first four axes of the PCA (Fig. 5). The difference is
286 especially true for env1 and env4, which are strongly associated with the first four
287 axes of the RDA, whereas PCA axes show an almost null correlation. The variables
288 env7, env8, env9 and env10 are also correlated to the first four axes of the RDA,
289 whereas PCs show far less correlation with these environments. Finally, RDA axes
290 show more correlation with the env3 and env6 variables than PCs (R^2 = ~0.30 vs R^2
291 = ~0). Furthermore, each RDA axis, from the first one to the fourth one, is associated
292 with more than one environmental variable, whereas only one PC (PC1) is
293 associated with env2 and env5 (Fig. S3).
294
295 Finally, over the 100 simulations, we measured the average FDR and power
296 for *pcadapt,* LFMM and RDA (Fig. 6). The three methods correctly identify almost all
297 of the QTL2 SNPs (Fig. 6A). RDA-based analysis and LFMM are more powerful than
298 *pcadapt* to identify QTL1 SNPs with, respectively, 75%, 48% and less than 10% of
299 true identification. For QTL3, *pcadapt* is not able to find any of the SNPs under
300 selection, whereas RDA reaches 24% of true identification and LFMM reaches 22%.

301 The three methods properly control for the false discovery rate because the
302 proportion of false discoveries obtained with *pcadapt*, LFMM and the RDA-based
303 methods are, respectively, 5%, 2.3% and 2.3% when controlling for a nominal error
304 rate of 5%.
305
306 **2. *Populus trichocarpa***
307 For the RDA and *pcadapt* analysis on the *P. trichocarpa* dataset, we retained
308 respectively *K*=3 and *K*=6 axes as indicated by the scree plots (Fig. S4) and we used
309 the two first axes of a PCA on environmental variables as composite variables for the
310 LFMM procedure (Fig. S5). Analysis with an FDR of 0.1 provides a list of 151 outliers
311 for RDA, 117 for *pcadapt* and 36 for LFMM. Interestingly, the three methods have
312 only 9 outliers in common and 117, 77 and 11 SNPs are outliers, respectively,
313 specific to RDA, *pcadapt* and LFMM.
314 When we compared RDA genome scan results with the outliers found by
315 Geraldes *et al.* (2014) based on Fdist, BayeScan and bayenv methods, we found a
316 substantial overlap between them (Fig. 7). Among the 151 outliers found with the
317 RDA-based method, 69 have already been picked up by *Fst*-based methods (see
318 Table S3). Interestingly, the loci showing the lowest p-values with the RDA analysis
319 are also pointed out as outliers by the *Fst* and *pcadapt* methods, but not by the
320 LFMM procedure (Fig. 7). However, the RDA-based genome scan found 72 SNPs that

321 no other methods, including *pcadapt*, detected as outliers.

322 When we performed a new RDA on the set of 151 outlier loci as detected by
323 the RDA-based genome scan method (adaptive enriched genetic space), we found
324 that the two first axes keep most (respectively 40% and 18%) of the adaptive
325 genetic variance among the populations (Fig. 8A). These two axes correspond to the
326 two principal selective pressures in the sampling area. RDA1 is correlated with
327 several environmental variables used in the analysis (Fig. 8A), including DD_0, DD18,
328 MAT, MCMT, and EMT, which correspond to temperature indexes. RDA1 is also
329 correlated to moisture variables (e.g., AHM or MAP), continentality (TD) and
330 flowering period length (bFFP and eFFP). This axis summarizes a gradient of global
331 climatic variation encountered in the sampling area with southern and coastal
332 populations opposed to northern and continental populations (Fig. 8B). On the other
333 side, RDA2 also correlates with moisture and temperature variables such as AHM,
334 MAP, TD, MCMT, and eFFP and contrasts individuals from coastal locations to
335 individuals from inland areas (Fig. 8C).

336

337 **DISCUSSION**

338 Genome scans based on genetic differentiation, as implemented in *pcadap*t,
339 detect true positives when environmental gradients related to adaption are
340 correlated to population structure. For instance, QTL2 SNPs are adaptive along an

341 environmental gradient that is correlated with population structure (see Fig. 2) and
342 they are detected by *pcadapt* (Fig. 6). By contrast, when the environmental gradient
343 is not correlated to population structure (QTL3 and QTL1 to a lesser extent) it fails
344 to detect adaptive SNPs. In this case, PCA ordination is not capable of orienting
345 genetic variation into the direction of environment 1 or 3. Fig. 6 shows that RDA has
346 a larger statistical power than *pcadapt* to detect QTL1 SNPs by taking advantage of
347 information from environmental local conditions. It can be attributed to a better
348 alignment between the genetic space and the environmental variable improving the
349 power to detect true positives. This better alignment is easily visible when looking at
350 the PCA and RDA correlation with environmental variables (Fig. 5 & Fig. S3). PCA is
351 only capable of identifying axes, which correspond to maximum genetic
352 differentiation (PC1 and PC2), whereas RDA is also able to capture the genetic
353 variability associated with other environmental variables, such as env1 (RDA3) and
354 to a lesser extent env3 (RDA4).
355
356 Genotype-environment approaches (GEA) explicitly take into account the
357 relationship between genotypes and the environment (Joost *et al.* 2007, de
358 Villemereuil *et al*. 2014, Lotterhos and Whitlock 2015). We showed that univariate
359 GEA, implemented in LFMM, and multivariate GEA, based on RDA, can show similar
360 results in identifying adaptive variation although RDA is more powerful than LFMM

361 for QTL1 SNPs (Fig. 6). As suggested in the literature, we limited the number of
362 environmental predictors during the LFMM procedure by using environmental PCA
363 axes as composite variables (Frichot *et al.*, 2013). We then only used the two first
364 PCs, but adding the third and fourth ones could potentially increase the capacity of
365 LFMM to detect QTL1 and QTL3 SNPs. It points out one of the advantages of a
366 multivariate procedure (e.g., RDA) compared to univariate GEA because multivariate
367 methods take all environmental variation into account at the same time and can
368 simultaneously detect associations between different sets of loci and different sets of
369 environmental variables (Forester *et al.,* 2017).
370
371 Both RDA and LFMM fail to detect QTL3 outliers in, respectively, 75% and
372 80% of the simulations (Fig. 6), possibly because of the additional difficulty in
373 detecting adaptive SNPs on a coarse environment compared to a smooth
374 environmental gradient as in environment 1 and 2. LFMM and the RDA-based
375 genome scan rely on linear association between the environment and allelic
376 abundance (0, 1 or 2). Patchy selective pressure, such as env3, is difficult to identify
377 with a correlative approach. Forester and colleagues (2015) already found that
378 heterogeneous environmental selection decreases the capacity of RDA to identify the
379 loci under selection. The strength of selection and the level of allelic dispersion
380 during the simulations strongly influence the statistical power of RDA; weak

381 selective strength and strong dispersion are the less favorable conditions (Forester
382 *et al.*, 2015). Nonetheless, our simulations plead in favor of using a constrained
383 ordination method when relevant environmental variables are available in order to
384 both orientate the ordination axis in the direction of environmental gradients and to
385 account for most of the environmental variation. This result confirms that
386 constrained ordination shows a superior combination of low false positive and high
387 true positives rates across all levels of selection (Forester *et al.*, 2017).

388 During our RDA-based procedure, we use Mahalanobis distances as a test
389 statistic to identify genetic variation significantly associated with environmental
390 gradients. This distance is computed based on the scores of more than one RDA axis
391 and can thus condense the information of several RDA axes in one statistic. Some
392 other studies have used different RDA-based statistics to identify the loci under
393 putative selection. They often used a value estimated independently for the different
394 RDA axes, such as the loadings of the loci along the axis (e.g., extreme squared
395 loadings for Latsky *et al.*, 2012) and considering a threshold such as ± 3 SD (Forester
396 *et al.*, 2017). Mahalanobis distances can capture complex selection patterns where
397 allelic variation depends on more than one environmental gradient. This statistic is
398 appropriate to identify selective pressures on natural populations, which usually
399 encompass multifactorial gradients of selection (Salmela, 2014).
400

401 One application of ordination methods is to detect selective gradients. The
402 RDA-based approach succeeded very well in decomposing the QTL SNPs-
403 environments associations along the different axes, at least in our simulations. In our
404 example, we succeeded in dissociating the outliers linked to the different
405 environmental variables, and thus to precisely identify which set of variables drives
406 each part of the adaptive genetic variability (Fig. 4). RDA1 is strongly associated with
407 env2, RDA2 with env7 (collinear with isolation by distance pattern in the grid),
408 RDA3 with env1 and RDA4 with env3. As expected, the correlated environments are
409 also strongly associated with these respective axes. This is reflecting the fact that it
410 is difficult to distinguish among several collinear variables which environmental
411 variable has a causal effect on the individual fitness. However, it is often sufficient to
412 identify the combination of environment variables having a strong association with
413 adaptive variation without precisely knowing the underlying mechanical process.
414 These simulations serve as a proof of concept to show that ordination axes can
415 provide holistic measures of genomic adaptation (Steane *et al.,* 2014). Under this
416 idea, scores of individuals on one RDA axis reflect their degree of adaptation along
417 this axis. RDA produces useful visualization of gradients of genetic adaptation (Fig.
418 8).
419
420 From the analysis of *Populus trichocarpa*, RDA found numerous outlier loci

421 (72) that are not detected by any other genome scan method, including *pcadapt* and
422 LFMM (Fig. 7 and Table S3). These results support the simulation analysis
423 conclusions that the RDA-based genome scan is able to pick up more genetic
424 markers in relation to environmental gradients than *pcadapt*. It is, however,
425 noticeable that a proportion of outliers are shared between PCA and RDA-based
426 methods (29), highlighting the fact that both approaches are partially similar. The
427 difficulty in interpreting the PCA axes is compensated by the fact that it is a blind
428 method in regard to environmental data, so it can pick up genes that we will miss
429 using RDA because some crucial environmental data are lacking. In the same vein,
430 half of the outlier loci found with the LFMM procedure (14 over 33 loci) are common
431 with RDA results (Fig. 7 and Table S3). The two methods rely on linear regression
432 between environmental and genetic variability, and by using PCs as composite
433 environmental variables in the LFMM procedure, we even add some similarity
434 between the two approaches.

435 After focusing the RDA analysis on the loci showing significant association
436 with environmental variables (151 outliers), we identified the predominant
437 environmental gradients structuring the genetic adaptation of *Populus trichocarpa.*
438 The main one is a composite climatic variation (RDA1 in Fig. 8), gathering
439 precipitation, temperature and seasonality variations. It clearly contrasts the
440 populations coming from the extreme northern part of the sampling area (Alaska)

441 and the population coming from the inland locations (higher altitudes) to the
442 populations close to the coast in British Columbia (Canada) and the southern
443 populations, near Portland, Oregon (USA). This result is in accord with the
444 conclusions of Geraldes *et al.* (2014). In their study, they point out the need of
445 adaptation to seasonality, photoperiod and frost events for *Populus trichocarpa*
446 along its continuous distribution from 44 to almost 60 degrees of latitude. RDA2 is
447 associated with moisture regimes and points out a gradient of adaptation between
448 coastal locations, strongly watered, and inland populations, receiving less
449 precipitation (Fig. 8). These two environmental gradients are the strongest selective
450 pressures driving *Populus trichocarpa* climatic adaptation in northwest America,
451 considering the set of environmental variables available and the scale of the analysis.
452 To go further, these composite indexes could also serve to predict (i) provenances
453 that would perform well in common gardens; (ii) patterns of adaptation to local
454 climate across the geographic range; or (iii) future adaptive landscapes in the
455 context of climate change.
456

457 **ACKNOWLEDGEMENTS**

458 We would like to dedicate this paper to the memory of our colleague and
459 beloved friend Eric Bazin (1977-2017) who passed away too soon.

460 TC acknowledges support from the ANR project APPATS (ANR-15-CE02-

0004) and MB acknowledges the Grenoble Alpes Data Institute, which is supported by the French National Research Agency under the "Investissements d'avenir" program (ANR-15-IDEX-02). MB also acknowledges support from the ANR project AGRHUM (ANR-14-CE02-0003-01).

REFERENCES

Bazin, Eric, Kevin J. Dawson, and Mark A. Beaumont. 2010. "Likelihood-Free Inference of Population Structure and Local Adaptation in a Bayesian Hierarchical Model." *Genetics* 185 (2): 587–602.

Coop, Graham, David Witonsky, Anna Di Rienzo, and Jonathan K. Pritchard. 2010. "Using Environmental Correlations to Identify Loci Underlying Local Adaptation." *Genetics* 185 (4): 1411–23.

Kort, Hanne De, Katrien Vandepitte, Hans Henrik Bruun, Déborah Closset-Kopp, Olivier Honnay, and Joachim Mergeay. 2014. "Landscape Genomics and a Common Garden Trial Reveal Adaptive Differentiation to Temperature across Europe in the Tree Species Alnus Glutinosa." *Molecular Ecology* 23 (19): 4709–21.

De Villemereuil, Pierre and Oscar E. Gaggiotti. 2015. "A New FST-Based Method to Uncover Local Adaptation Using Environmental Variables." *Methods in Ecology and Evolution* 6 (11): 1248–58. doi:10.1111/2041-210X.12418.

Duforet-Frebourg, Nicolas, Keurcien Luu, Guillaume Laval, Eric Bazin, and Michael G B Blum. 2016. "Detecting Genomic Signatures of Natural Selection with Principal Component Analysis: Application to the 1000 Genomes Data." *Molecular Biology and Evolution* 33 (4): 1082–93.

Foll, Matthieu, and Oscar Gaggiotti. 2008. "A Genome-Scan Method to Identify Selected Loci Appropriate for Both Dominant and Codominant Markers: A Bayesian Perspective." *Genetics* 180 (2): 977–93.

Forester, Brenna R, Jesse R Lasky, Helene H Wagner, and Dean L Urban. 2017. "Comparing Methods for Detecting Multilocus Adaptation with Multivariate Genotype," no. 970: 1–42.

Forester, Brenna R., Matthew R. Jones, Stéphane Joost, Erin L. Landguth, and Jesse R. Lasky. 2016. “Detecting Spatial Genetic Signatures of Local Adaptation in Heterogeneous Landscapes.” *Molecular Ecology* 25 (1): 104–20.

François, Olivier, Helena Martins, Kevin Caye and Sean D. Schoville. 2016. "Controlling false discoveries in genome scans for selection." *Molecular Ecology* 25 (2): 454-469.

Frichot, Eric, Sean D. Schoville, Guillaume Bouchard, and Olivier François. 2013. “Testing for Associations between Loci and Environmental Gradients Using Latent Factor Mixed Models.” *Molecular Biology and Evolution* 30 (7): 1687–99.

Geraldes, A., S. P. Difazio, G. T. Slavov, P. Ranjan, W. Muchero, J. Hannemann, L. E. Gunter, et al. 2013. “A 34K SNP Genotyping Array for Populus Trichocarpa: Design, Application to the Study of Natural Populations and Transferability to Other Populus Species.” *Molecular Ecology Resources* 13 (2): 306–23.

Geraldes, Armando, Nima Farzaneh, Christopher J. Grassa, Athena D. Mckown, Robert D. Guy, Shawn D. Mansfield, Carl J. Douglas, and Quentin C B Cronk. 2014. “Landscape Genomics of Populus Trichocarpa: The Role of Hybridization, Limited Gene Flow, and Natural Selection in Shaping Patterns of Population Structure.” *Evolution* 68 (11): 3260–80.

Hecht, Benjamin C., Andrew P. Matala, Jon E. Hess, and Shawn R. Narum. 2015. “Environmental Adaptation in Chinook Salmon (Oncorhynchus Tshawytscha) throughout Their North American Range.” *Molecular Ecology* 24 (22): 5573–95.

Hoban, Sean, Joanna L. Kelley, Katie E. Lotterhos, Michael F. Antolin, Gideon Bradburd, David B. Lowry, Mary L. Poss, Laura K. Reed, Andrew Storfer, and Michael C. Whitlock. 2016. “Finding the Genomic Basis of Local Adaptation: Pitfalls, Practical Solutions, and Future Directions.” *The American Naturalist* 188 (4): 379–97.

Lasky, Jesse R., David L. Des Marais, John K. McKay, James H. Richards, Thomas E. Juenger, and Timothy H. Keitt. 2012. “Characterizing Genomic Variation of Arabidopsis Thaliana: The Roles of Geography and Climate.” *Molecular Ecology* 21 (22): 5512–29.

Legendre, Pierre, and Louis Legendre. 1988. “Numerical Ecology, Volume 24.” *(Developments in Environmental Modelling)* 24: 870.

Luu, Keurcien, Eric Bazin, and Michael G B Blum. 2017. “Pcadapt: An R Package to Perform Genome Scans for Selection Based on Principal Component Analysis.” *Molecular Ecology Resources* 17 (1): 67–77.

Martins, Helena, Kevin Caye, Keurcien Luu, Michael G.B. Blum, and Olivier François. 2016. “Identifying Outlier Loci in Admixed and in Continuous Populations Using Ancestral Population Differentiation Statistics.” *Molecular Ecology* 25 (20): 5029–42.

Oksanen, Jari, F Guillaume Blanchet, Michael Friendly, Roeland Kindt, Pierre Legendre, Dan Mcglinn, Peter R Minchin, et al. 2015. “Vegan: Community Ecology Package.” *R Package Version 2.3-2*, https://CRAN.R-project.org/package=vegan.

Peng, Bo, and Marek Kimmel. 2005. “simuPOP: A Forward-Time Population Genetics Simulation Environment.” *Bioinformatics* 21 (18): 3686–87.

Pritchard, Jonathan K., and Anna Di Rienzo. 2010. “Adaptation - Not by Sweeps Alone.” *Nature Reviews Genetics* 11 (10). Nature Publishing Group: 665–67.

Salmela, Matti J. 2014. “Rethinking Local Adaptation: Mind the Environment!” *Forest Ecology and Management* 312. Elsevier B.V.:271–81.

Savolainen, Outi, Martin Lascoux, and Juha Merilä. 2013. “Ecological Genomics of Local Adaptation.” *Nature Reviews Genetics* 14 (11): 807–20.

Steane, Dorothy A., Brad M. Potts, Elizabeth McLean, Suzanne M. Prober, William D. Stock, René E. Vaillancourt, and Margaret Byrne. 2014. “Genome-Wide Scans Detect Adaptation to Aridity in a Widespread Forest Tree Species.” *Molecular Ecology* 23 (10): 2500–2513.

Storey, John D. and Andrew J. Bass. 2011. “Bioconductor’s Qvalue Package.” *Gene*, no. 2001: 1–6.

Vangestel, Carl, Andrew J. Eckert, Jill L. Wegrzyn, J. Bradley St. Clair, and David B. Neale. 2018. “Linking Phenotype, Genotype and Environment to Unravel Genetic Components Underlying Cold Hardiness in Coastal Douglas-Fir (Pseudotsuga Menziesii Var. Menziesii).” *Tree Genetics & Genomes* 14 (1). Tree Genetics & Genomes:10.

Vatsiou, Alexandra I., Eric Bazin, and Oscar E. Gaggiotti. 2016. “Detection of Selective Sweeps in Structured Populations: A Comparison of Recent Methods.” *Molecular Ecology* 25 (1): 89–103.

Wang, Jiahui, Ruben Zamar, Alfio Marazzi, Victor Yohai, Matias Salibian-Barrera, Ricardo Maronna, Eric Zivot, et al. 2014. “Robust: Robust Library.” *R Package Version 0.4-16*. http://cran.r-project.org/package=robust.

Whitlock, Michael C., and Katie E. Lotterhos. 2015. “Reliable Detection of Loci Responsible for Local Adaptation: Inference of a Null Model through Trimming the Distribution of F_{ST}.” *The American Naturalist* 186 (S1): S24–36.

Yang, Wen Yun, John Novembre, Eleazar Eskin, and Eran Halperin. 2012. “A Model-Based Approach for Analysis of Spatial Structure in Genetic Data.” *Nature Genetics* 44 (6): 725–31.

556 # DATA ACCESSIBILITY STATEMENT

557 • Simulations datasets are available at the Dryad Digital Repository at the
558 following address:
559 https://datadryad.org/review?doi=doi:10.5061/dryad.1s7v5
560
561 • Scripts used for simulations and *Populus trichocarpa* analysis are available on
562 Github: https://github.com/Capblancq/RDA-genome-scan
563
564 • *Populus trichocarpa* SNP data are available on Dryad:
565 http://datadryad.org/resource/doi:10.5061/dryad.1051d
566

567 # AUTHOR CONTRIBUTIONS

568 E. Bazin designed the study. E.B. and T. Capblancq performed the analysis and
569 treatments. M. Blum, E.B. and T.C. wrote the manuscript, and all authors contributed
570 substantially to revisions.
571

572 # TABLES AND FIGURES

573 **Figure 1:** Schematic representation of the RDA-based procedure for searching loci
574 under selection.

575 **Figure 2:** Graphical representations of mean environmental values for
576 environments 1 to 10. Equation determining the environment is given in the main
577 manuscript. Mean environmental values for environments 4, 5 and 6 are,
578 respectively, equivalent to environments 1, 2 and 3.

579 **Figure 3:** Manhattan plots of the results obtained with *pcadapt* (upper left panel),
580 RDA (upper right panel), and LFMM (lower panels) for one simulated dataset.

581 **Figure 4:** Projection of SNPs and environmental variables into the RDA space.

582 **Figure 5:** Proportion of environmental variance explained by the first four
583 ordination axes using RDA or PCA. The values correspond to the r-squared of the
584 regression between the environmental variable and the first four axes of the
585 multivariate analysis.

586 **Figure 6:** Statistical power obtained with RDA, *pcadapt*, and LFMM. Estimate of
587 power corresponds to an average over 100 simulated datasets (error bars are
588 displayed). Power (A) is given separately for loci coding for quantitative traits 1, 2
589 and 3. False Discovery Rate (FDR) is given for all methods (B).

590 **Figure 7:** Scatter plot of the p-values returned by RDA and *pcadapt* procedures (A)
591 and the p-values returned by RDA and LFMM procedure (B) for the *Populus*
592 *trichocarpa* dataset. Black dots correspond to loci identified as outliers by *Fst*
593 methods in Geraldes *et al*. (2014). The dashed lines indicate a 10-3 p-value with RDA
594 and *pcadapt* or LFMM.

595 **Figure 8:** Projection of SNPs and environmental variables in the RDA performed on
596 the adaptively enriched genetic space (151 loci) of *P. trichocarpa* dataset (A). The
597 first two axes of the RDA projection represent 40% (RDA1) and 18% (RDA2) of the
598 explained variance. (B) and (C) show respective spatial representations of RDA1 and
599 RDA2 axes scores in the sampling area. The points represent the 133 sampled
600 populations and their color depends on the mean of individual RDA1 (B) and RDA2
601 (C) scores in the populations.

602

603 **SUPPORTING INFORMATION**

604 **Script S1:** Detailed script of the RDA-based genome scan analysis.

605 **Table S1:** Environmental variables used in the *Populus trichocarpa* analysis.

606 **Table S2:** Climatic variable values for the 133 *Populus trichocarpa* sampled
607 populations.

608 **Table S3:** Comparison between RDA, *pcadapt*, *fdist* and *bayescan* outlier loci.

609 **Figure S1:** Scree plot for PCA and RDA analysis of the simulation 1 dataset.

610 **Figure S2:** PCA and scree plot of PCA on environmental variables of the first
611 simulation.

612 **Figure S3:** Heatmap of the R^2 resulting from linear regression between the four first
613 axes of PCA and RDA analysis and the environmental variables.

614 **Figure S4:** Scree plot for PCA and RDA analysis of *Populus trichocarpa* dataset.

615 **Figure S5:** PCA and scree plot of PCA on environmental variables of the *Populus*
616 *trichocarpa* dataset.

617

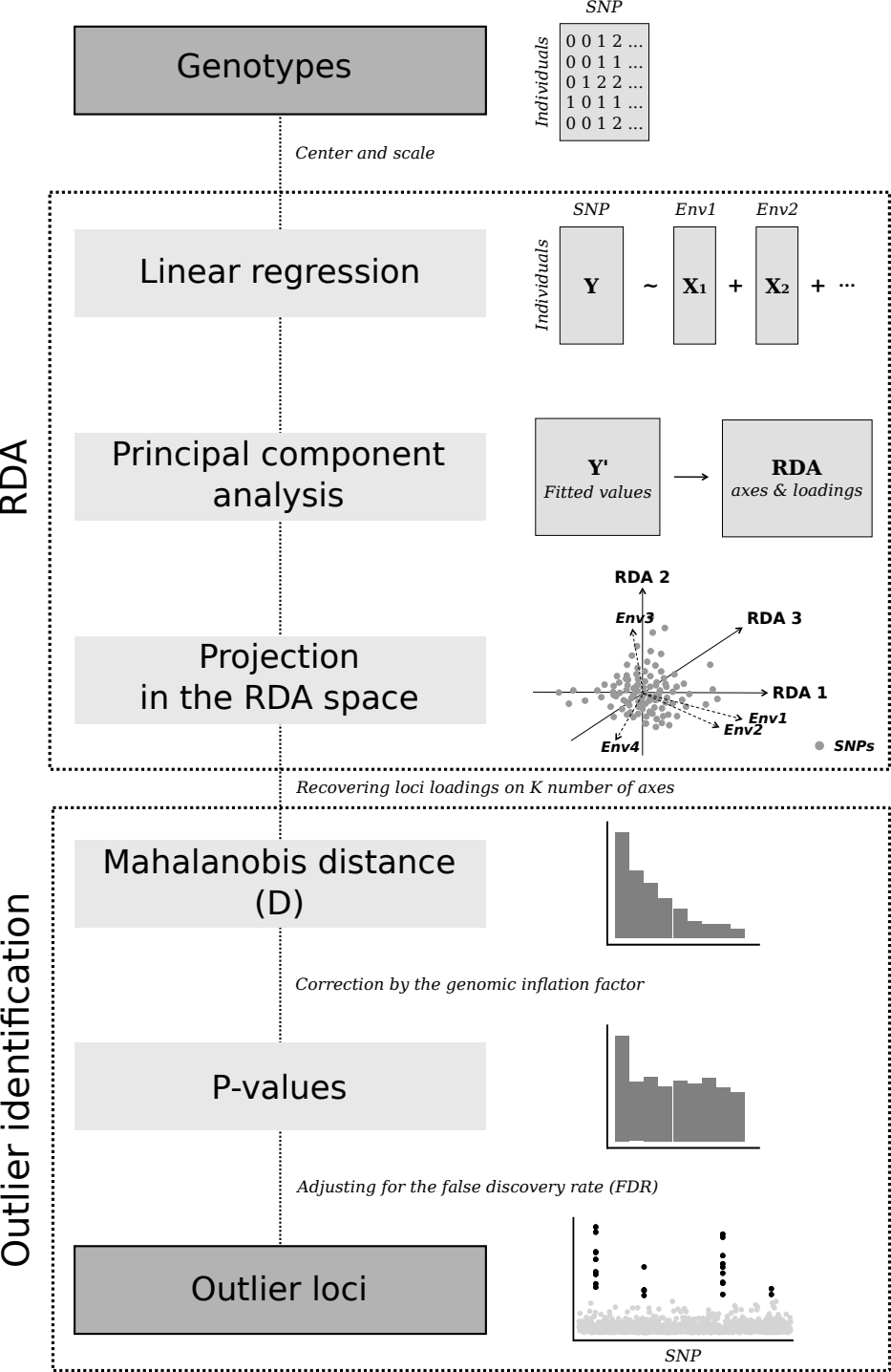
Genotypes
SNP
Individuals
0 0 1 2 ...
0 0 1 1 ...
0 1 2 2 ...
1 0 1 1 ...
0 0 1 2 ...
Center and scale
RDA
Linear regression
SNP
Env1
Env2
Individuals
Y
~
X1
+
X2
+ ···
Principal component analysis
Y'
Fitted values
RDA
axes & loadings
Projection in the RDA space
RDA 2
Env3
RDA 3
RDA 1
Env1
Env2
Env4
SNPs
Recovering loci loadings on K number of axes
Outlier identification
Mahalanobis distance (D)
Correction by the genomic inflation factor
P-values
Adjusting for the false discovery rate (FDR)
Outlier loci
SNP

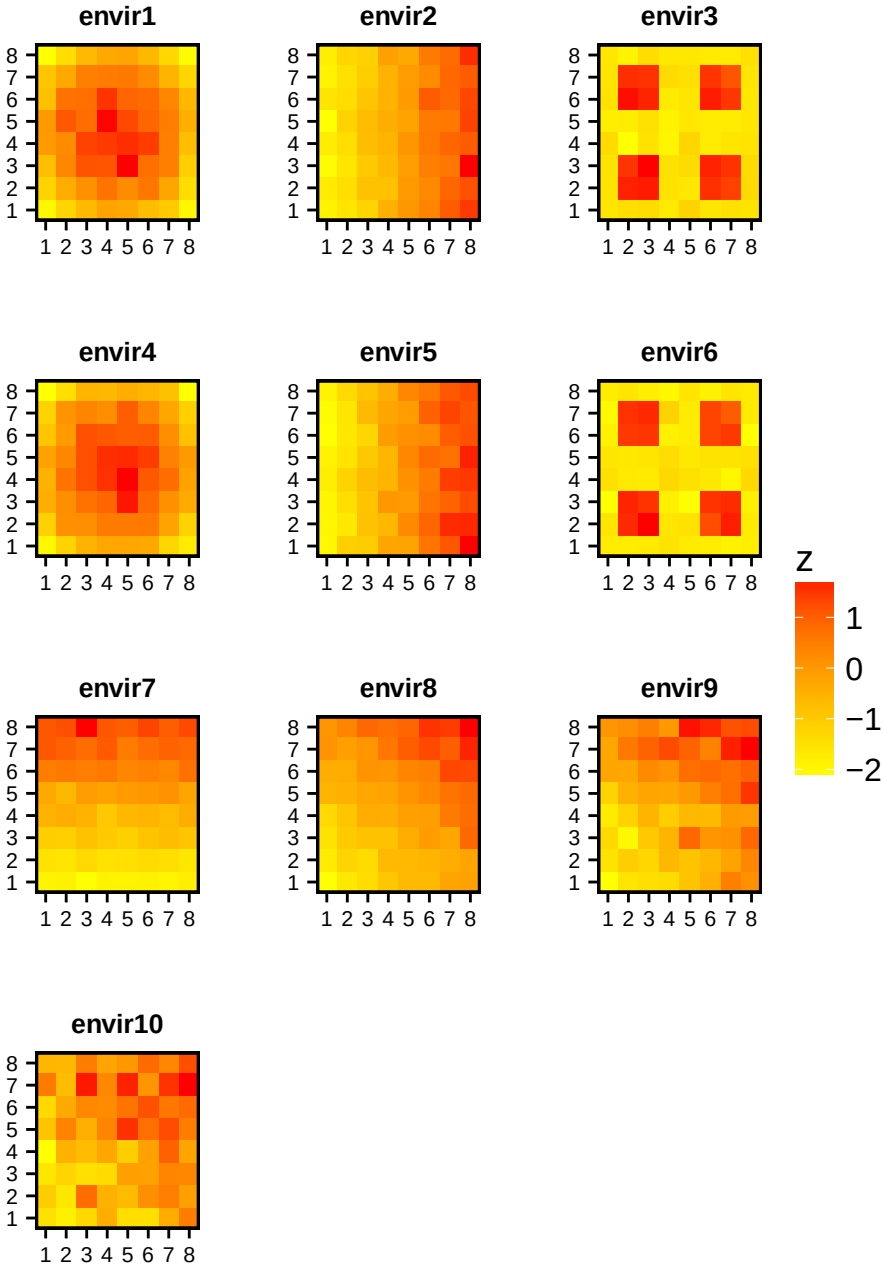
envir1
envir2
envir3
envir4
envir5
envir6
envir7
envir8
envir9
envir10
1 2 3 4 5 6 7 8
z
1
0
−1
−2

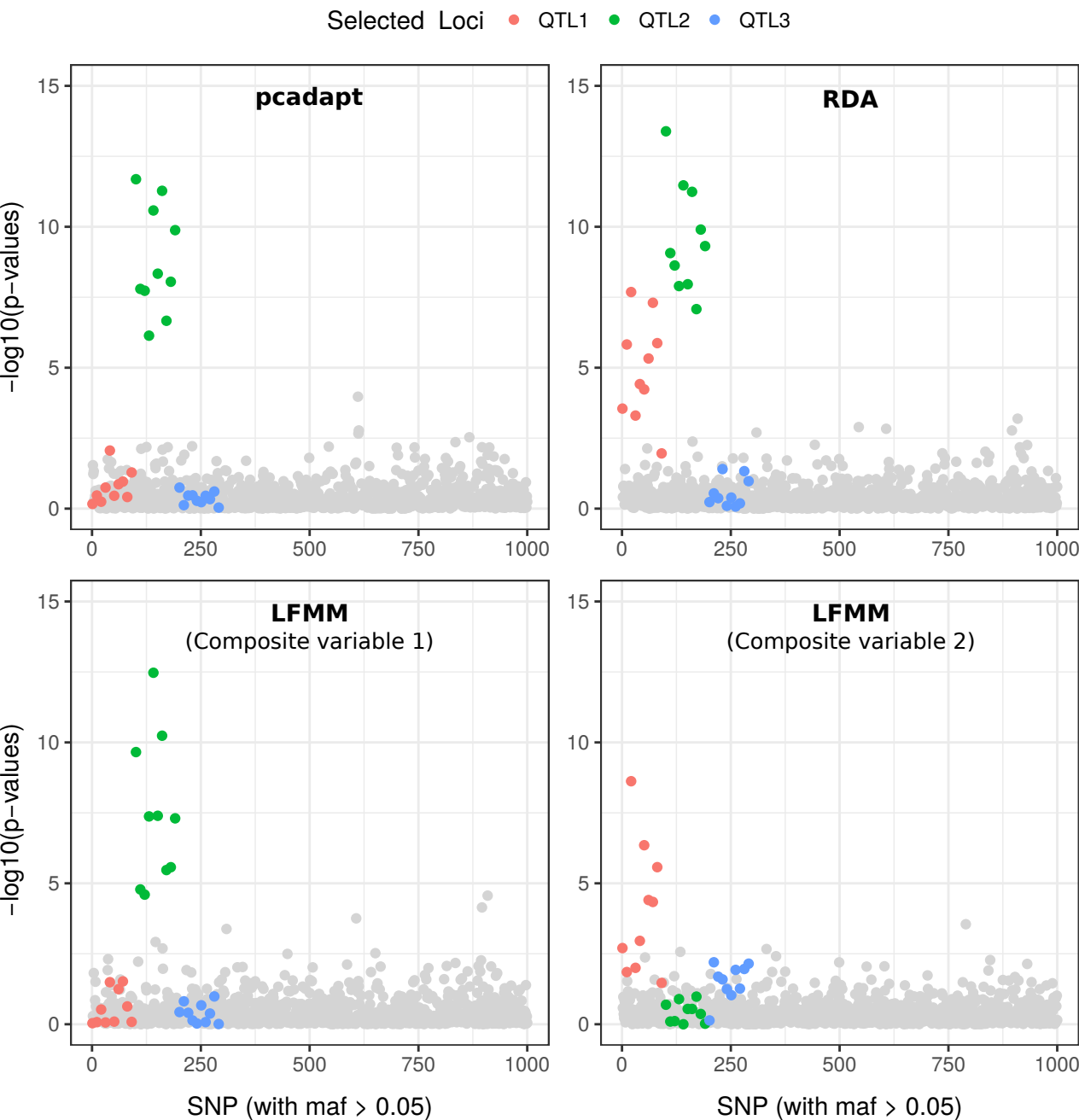
Selected Loci
QTL1
QTL2
QTL3
pcadapt
RDA
LFMM
(Composite variable 1)
LFMM
(Composite variable 2)
−log10(p−values)
SNP (with maf > 0.05)
0
5
10
15
0
250
500
750
1000

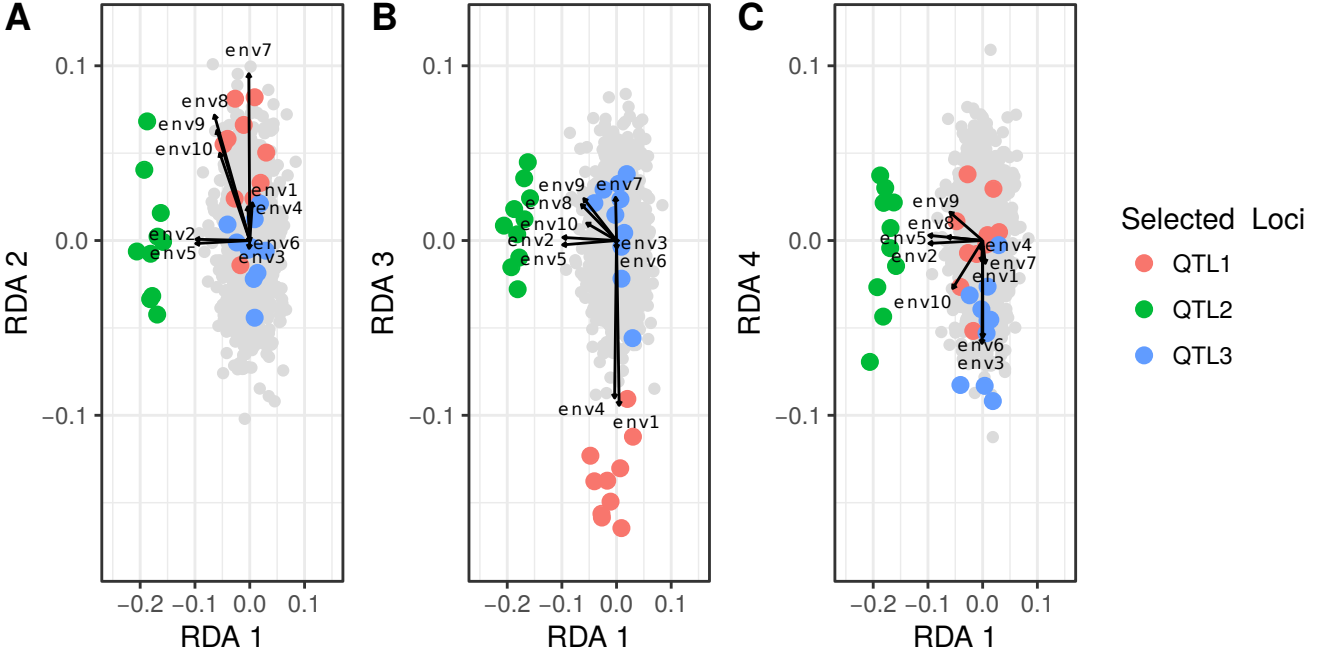
A
B
C
RDA 1
RDA 2
RDA 3
RDA 4
0.1
0.0
−0.1
−0.2
env1
env2
env3
env4
env5
env6
env7
env8
env9
env10
Selected Loci
QTL1
QTL2
QTL3

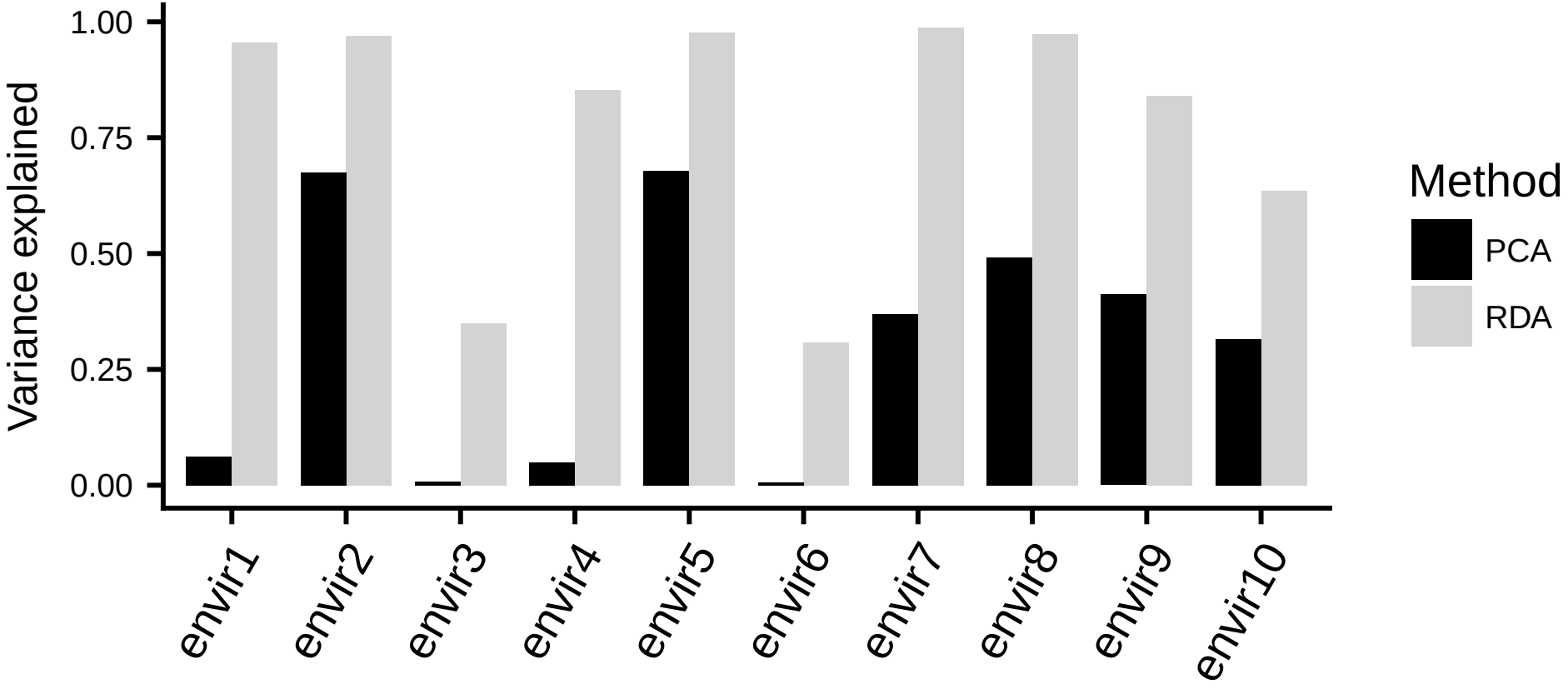
Variance explained
1.00
0.75
0.50
0.25
0.00
envir1
envir2
envir3
envir4
envir5
envir6
envir7
envir8
envir9
envir10
Method
PCA
RDA

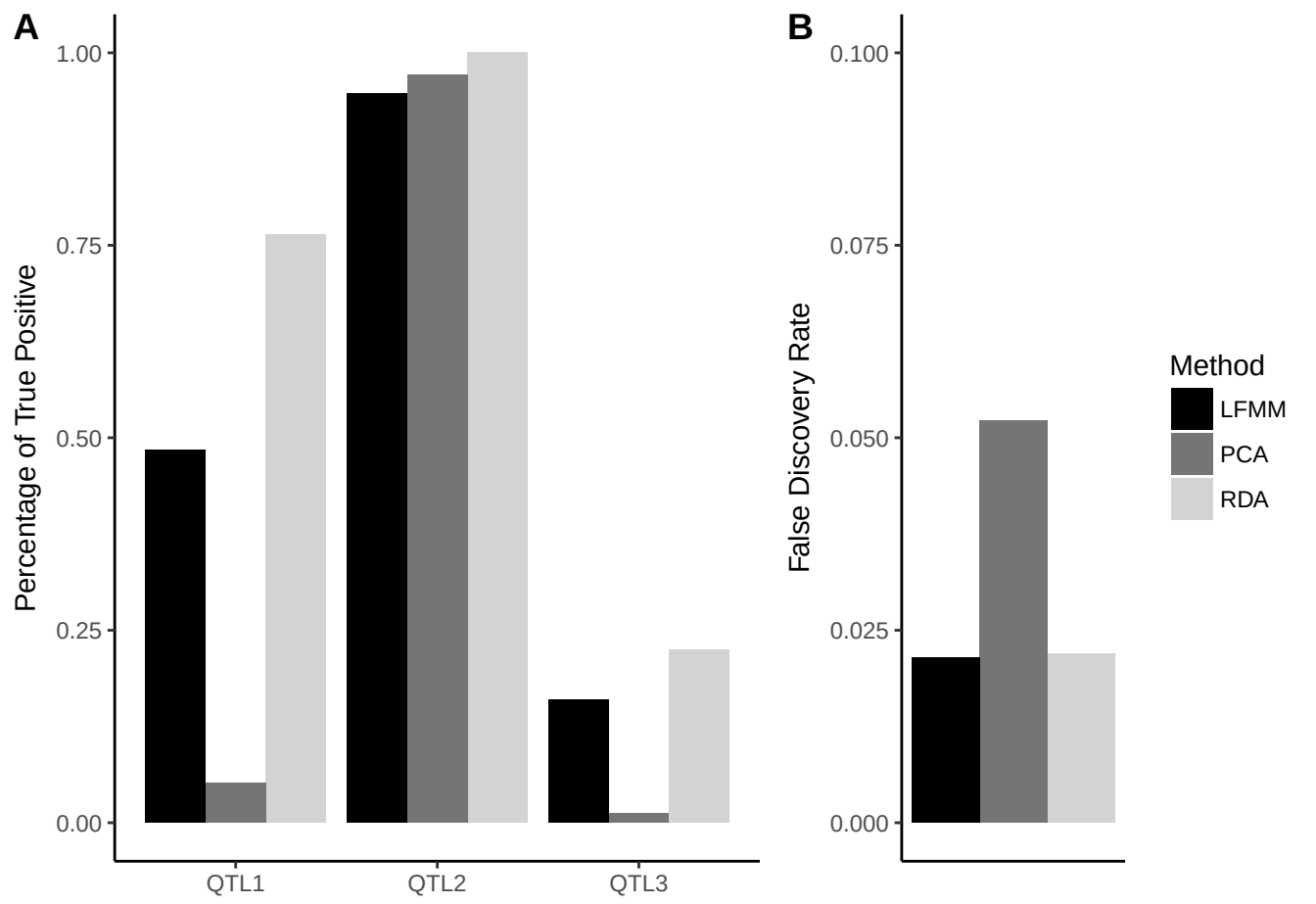
A
B
Percentage of True Positive
1.00
0.75
0.50
0.25
0.00
QTL1
QTL2
QTL3
False Discovery Rate
0.100
0.075
0.050
0.025
0.000
Method
LFMM
PCA
RDA

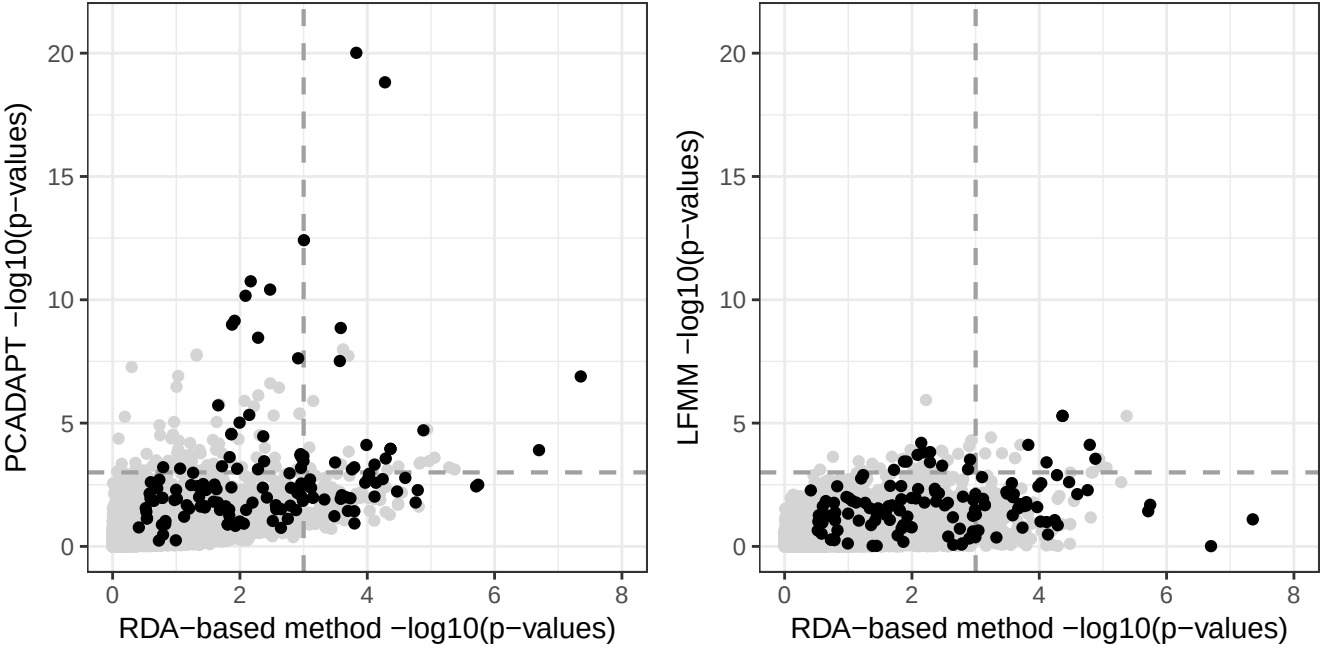
PCADAPT −log10(p−values)
RDA−based method −log10(p−values)
LFMM −log10(p−values)
RDA−based method −log10(p−values)
0
5
10
15
20
0
2
4
6
8

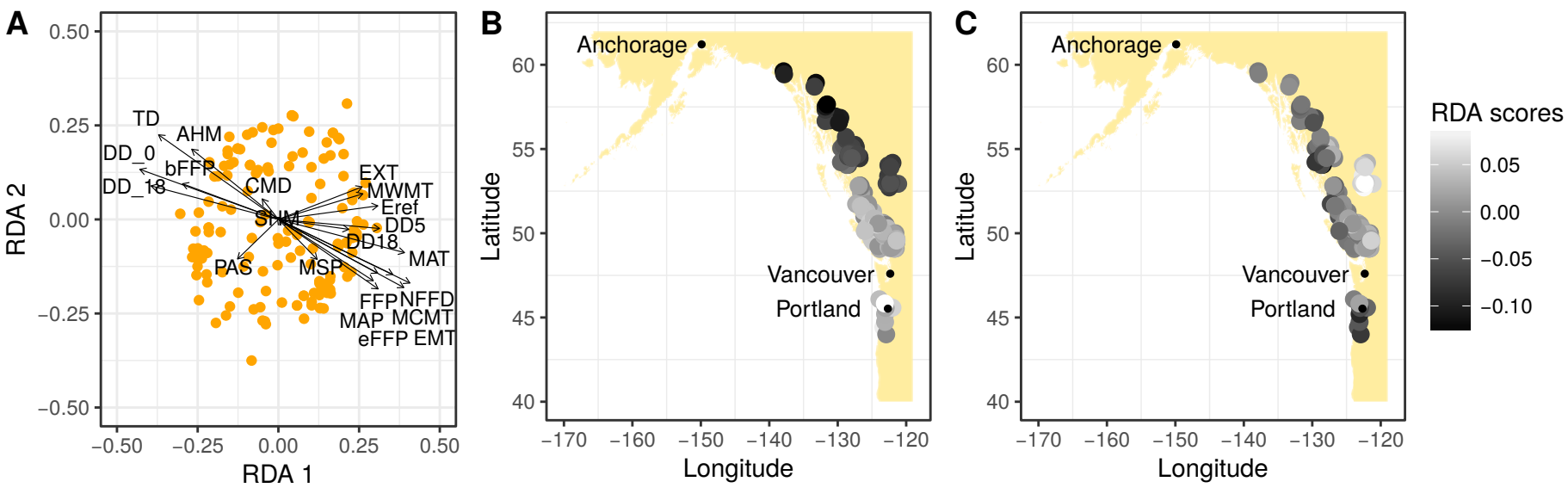
A
B
C
RDA 1
RDA 2
TD
AHM
DD_0
bFFP
DD_18
CMD
EXT
MWMT
Eref
SHM
DD5
DD18
MAT
PAS
MSP
FFP
NFFD
MAP
MCMT
eFFP
EMT
Anchorage
Vancouver
Portland
Latitude
Longitude
RDA scores
0.05
0.00
−0.05
−0.10